

Monte Carlo study of structure and kinetics of formation of end-linked polymer networks

A.G. Balabanyan^{a,*}, E.Yu. Kramarenko^{a,b}, I.A. Ronova^b, A.R. Khokhlov^{a,b}

^aPhysics Department, Moscow State University, Leninskie Gory, Moscow 119992, Russia

^bNesmeyanov Institute of Organoelement Compounds, Russian Academy of Science, Vavilova str. 28, Moscow 119991, Russia

Available online 17 March 2005

Abstract

The kinetics of formation and structural properties of end-linked polymer networks were studied by Monte Carlo simulations on a three-dimensional cubic lattice. Networks were generated from the solutions of linear polymer chains with functional end groups and tetrafunctional cross linkers. Systems of 10-, 20-mer precursor polymer chains with values of the ratio of cross linkers to polymer chains end groups r ranging from 0.9 to 1.4 were studied. Polymer volume fraction ϕ was varied from 0.1 to 0.5. Different ways of polymer network formation are possible, namely, gel creation process can proceed as homogeneous gelation as well as microgel separation. In addition to those limiting ways of polymerization process, intermediate cases were observed. All varied parameters (length of precursor polymer chains N , r and ϕ) influence the kinetics of the cross-linking. An algorithm to determine the soluble fraction in solution and the amount of loops and pendent structures in the polymer network was proposed. In agreement with experimental observations, simulations show that networks with lower soluble fractions which are more defect-free result from long precursor polymer chains ($N=20$) for approximately polymer melt densities ($\phi \approx 0.4$) at higher than stoichiometric r values ($r \approx 1.2$).

© 2005 Published by Elsevier Ltd.

Keywords: Polymer networks; Kinetics of gelation; Microscopic structure

1. Introduction and overview

Polymer networks [1] are the basic structural elements of such different systems as tire rubbers and gels. They are encountered not only in technical applications, but also in biological systems (for example in cytoskeleton). The molecular architecture of polymer networks strongly influences their mechanical and chemical behavior [2,3]. That is why many research works are carried out in order to establish the relations between conditions of networks synthesis and their microscopic structure. A considerable contribution to the area of the physical chemistry of polymer networks was made by Professor J. E. Mark and his co-workers. In particular, many of his studies concern elasticity of polymer networks [4–8]. Numerous significant results were obtained by extensive computer simulation studies of elastomers and rubberlike elasticity [9–12].

Computer simulations offer various important advantages over experimental and theoretical research. One can mention greater freedom and control over the formation of networks or access to the microscopic structure and dynamics. Simple simulation models, such as bond or site percolations are not applicable, since cross-links that are topologically nearest neighbors are not necessarily nearest neighbors in space and vice versa. That is why we used Monte Carlo computer simulations to study the structure of networks as well as the kinetics of their formation.

We simulated the system of short linear end-functionalized polymer chains and tetrafunctional cross linkers. The cross-linking reaction was allowed only between an unreacted chain end and unsaturated cross-linker. An ideal, model end-linked network corresponds to the situation when all precursor polymer chains become elastic ones [13]. In real networks, however, imperfections cause the elastic properties to diminish. These imperfections include pendent structures, which are attached to the network by only one end, and loops. In the present paper we study the resulting network molecular architecture with such methods that allow to calculate the sol fraction [14] and the amount of pendent material and loops [15]. Our aim

* Corresponding author. Tel.: +7 95 9391013; fax: +7 95 9392988.
E-mail address: balab@polly.phys.msu.ru (A.G. Balabanyan).

was to determine conditions that minimized the amount of sol fraction and network defects.

In this work we study the influence of the following parameters on the cross-linking process: the ratio of the number of cross-linker sites divided by the number of chain ends available for reaction, r , length of precursor polymer chains, N and the volume fraction, ϕ . In some previous simulation studies [16,17] the volume fraction was held constant close to approximately polymer melt density. In our study the value of ϕ is varied in a wide range, like it was done in Ref. [18], in which the authors investigate the effect of entanglements on the network elastic response.

Another problem, addressed in this paper, is the way of polymer network formation. Among two opposite limiting ways of gel formation, which are homogeneous gelation and microgel separation, we have observed a number of intermediate cases. No correlations between gel point position and the way of network formation process were found. Furthermore, gel creation process is most likely to resemble homogeneous gelation and only in rare cases microgel separation was observed.

The rest of this paper is organized as follows. In Section 2, we describe the model and methods of simulation. In Section 3 we briefly explain how initial configurations of the modeled systems are created. Section 4 discusses kinetics of the cross-linking process. In Section 5 we present our results on the influence of conditions of network synthesis on the network formation process. Section 6 concerns structural properties of the resulting networks. Section 7 then summarizes our conclusions.

2. Model and simulation methodology

Polymer networks were simulated with the use of the bond-fluctuation model (BFM) [19,20] on a three-dimensional cubic lattice. One monomer unit of precursor chains as well as a cross-linker molecule occupies one lattice site and other monomer units are not allowed to occupy either this site or its nearest environment (i.e. 26 neighboring sites in 3d space). The set of allowed bond vectors connecting two successive monomer units is constructed to ensure non-intersection of bonds and the excluded volume of the monomer units. One possible choice for the bond vectors (utilized in our work) is a set of 108 different vectors with the lengths equal to 2, $\sqrt{5}$, $\sqrt{6}$, 3, $\sqrt{10}$ lattice spacings.

The dynamics is realized by choosing randomly, for each time step, a monomer unit or a cross-linker and an attempt to displace it to one of the six nearest lattice sites chosen with equal probability. The unit is moved to the new position, if the self-avoidance conditions are obeyed and the new bond vector is in the set of allowed bond vectors. Otherwise, the trial is discarded. Thus, we study the networks in an athermal approach where only excluded volume interactions and connectivity between repeat units are considered. It is possible to use such simple model since we are interested

only in structural properties of the networks and in general features of kinetics of their formation.

The cross-linker molecules have functionality equal to 4, i.e. one such molecule can react with maximum four chain ends. The reaction between a chain-end and a cross-linker was modeled as follows. Whenever an unreacted chain-end and a not fully reacted cross-linker move into nearest-neighbor positions (2 lattice spacings), a reaction takes place with a probability k . The value of k can be varied to model different reaction constants [21]. In our work it was set to unity. If a new bond is created it has to be in the set of allowed bond vectors at every future move, like the bond vectors in precursor chains.

3. Initial configuration

In the present study we used $123 \times 123 \times 123$ lattice for all simulated systems. The case when we studied kinetics of network formation in details was the only exception. In this case lattice had $246 \times 246 \times 246$ dimensions. Periodic boundary conditions were not imposed. The volume fraction of monomer units of precursor chains and cross-linker molecules in the system is defined as:

$$\phi = \frac{8v(NM + C)}{V}, \quad (1)$$

where N is the number of monomer units per precursor chain, M is the number of precursor chains, C is the number of cross-linkers, v is the volume of a lattice site, V is the lattice volume, and the factor 8 appears because each molecule occupies eight lattice sites.

For tetrafunctional end-linked systems the ratio, r , of the number of cross-linker sites available for reaction to the number of precursor polymer chains ends is defined as $r = 2C/M$. Both the 10-mer and the 20-mer networks were generated with various values of the volume fraction of monomer units of precursor chains and cross-linker molecules such as $\phi = 0.1, 0.2$ and 0.3 , corresponding to polymer solutions and $\phi = 0.4$ and 0.5 that approach polymer melts densities. For all of the chains lengths and ϕ values the simulations were performed at various values of r : $r = 0.9$ corresponding to the lack of cross-linker molecules; $r = 1.0$ for stoichiometric mixture composition; $r = 1.2$ and 1.4 corresponding to an excess of cross-linkers.

Solutions or melts of mono-disperse chains and tetrafunctional cross-linkers were prepared applying the following algorithm. At the first step the required amount of short precursor polymer chains for a given ϕ value were regularly distributed in the simulation box so that the possible maximum number of them could fit into the simulation cell with the account of the excluded volume and non-intersection conditions. As a result of this procedure we obtained an ordered array of stretched chains. Finally the cross-linker molecules were inserted randomly. This procedure was introduced, since it was impossible to create

initial configurations by placing randomly precursor polymer chains and cross-linkers for dense systems ($\phi \geq 0.4$). For lower densities ($\phi < 0.4$) an insertion of random conformations of chains is possible, but it is too time consuming.

After that the system was allowed to evolve in time until all the components of the radius of gyration

$$S = \frac{1}{N} \sum_{i=1}^N (\vec{r}_i - \vec{r}_0)^2,$$

where

$$\vec{r}_0 = \frac{1}{N} \sum_{i=1}^N \vec{r}_i$$

is the center of gravity of the polymer chain) of initially stretched and ordered chains were equilibrated. Moreover spatial distributions of monomer units and cross-linkers were calculated in order to check their homogeneity. During the equilibration phase no reaction was allowed to occur. As usual, the conventional time is measured in Monte Carlo micro-steps (MCMS), i.e. in the number of elementary moves (an attempt to relocate a particle to one of the six nearest neighbor positions). In the following simulations the duration of the equilibration period was equal to 1×10^{11} MCMS for all modeled systems.

Figs. 1 and 2 represent spatial distributions of the polymer chain units and cross-linkers calculated for the final configurations of the modeled system, consisting of 20-mer precursor polymer chains, with $r = 1.4$ and $\phi = 0.5$, in order to check its homogeneity. To obtain these dependences we have averaged both distributions over the thousand system configurations separated by 10^5 MCMS after the equilibration process passed (MCMS = 1×10^{11}). As the equilibration process goes, the cross-linker molecules diffuse through the sample, while precursor polymer chains bend

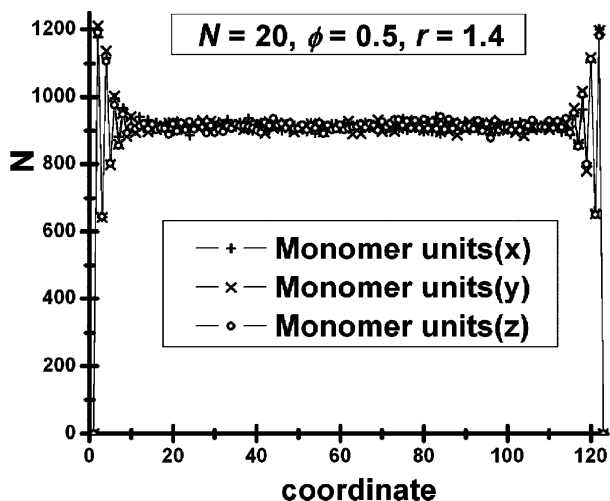


Fig. 1. Spatial distributions of the monomer units in the final configuration (MCMS = 1×10^{11}) of the equilibration phase for the simulated system, consisting of 20-mer precursor polymer chains with $r = 1.4$ and $\phi = 0.5$.

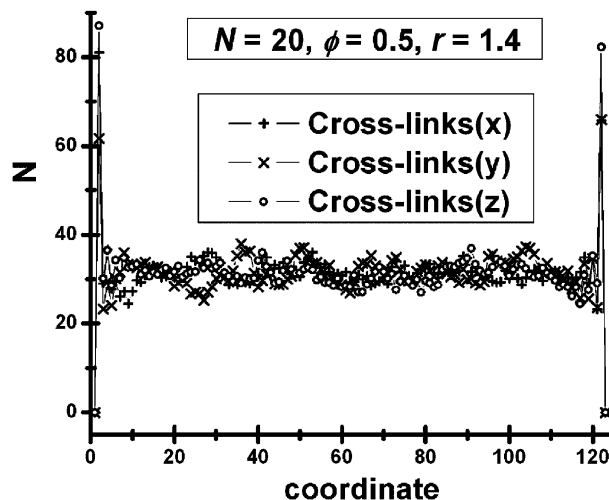


Fig. 2. Spatial distributions of the cross-linkers in the final configuration (MCMS = 1×10^{11}) of the equilibration phase for the simulated system, consisting of 20-mer precursor polymer chains with $r = 1.4$ and $\phi = 0.5$.

and distribute over the cell. Homogeneous distributions in Figs. 1 and 2 of both precursor polymer chain units and cross-linkers show that the equilibration period was long enough for chains to mix up and for the cross-linkers to diffuse through the simulation box. Final configurations of the equilibration phase for all modeled systems were checked to meet these requirements. One should mention that for all modeled systems we have checked that the mean squared displacement of cross-linker and the center of gravity of the polymer chains were not less than the half of the length of the simulation box.

4. Kinetics of the cross-linking process

Typical parameters calculated for the cross-linking process are the following:

1. Fraction of unreacted chain-ends. As a function of time it is expressed as follows: $b(t)/b(0)$, with $b(t) = b(0) - c_1 - 2c_2 - 3c_3 - 4c_4$ where c_i is the concentration of the cross-links with i chain-ends attached to them and b is the concentration of free chain-ends. The initial conditions are $c_i = 0$ for $i = 1, 2, 3, 4$ and in the stoichiometric case $4c_0 = b(0)$;
2. Conversion of the reacting solution p . It is defined as $p = 1 - N_{\text{mol}}(t)/N_{\text{mol,initial}}$, where $N_{\text{mol}}(t)$ is the number of molecules in the modeled system at the time t after the reaction was started and $N_{\text{mol,initial}}$ is the initial number of molecules in the simulation box. At $t = 0$ the value of p is equal to zero. As the cross-linking process goes the number of molecules in the system ($N_{\text{mol}}(t)$) decreases, since different chains are linked together to form new larger molecules. Thus p increases in time approaching its greatest possible value, which is equal to 1;
3. Number of segments in the largest molecule of the

reacting solution normalized with the total mass of the modeled system, what is the ratio between the mass (number of segments) of the largest molecule and the total mass (number of monomer units of precursor chains as well as a cross-linker molecules) of the modeled system;

4. Weight-average degree of polymerization including (P_w) and excluding ($P_{w,\text{sol}}$) the largest molecule. P_w and $P_{w,\text{sol}}$ are expressed as

$$P_w = \frac{\sum_{i=1}^{N_{\text{mol}}} l_i^2}{\sum_{i=1}^{N_{\text{mol}}} l_i} \text{ and } P_{w,\text{sol}} = \frac{\sum_{i=1}^{N_{\text{mol}}'} l_i^2}{\sum_{i=1}^{N_{\text{mol}}'} l_i},$$

where N_{mol} is the current number of molecules in the system and l_i is the number of monomer units in each molecule. These formulas differ only in the range of summation: in P_w the summation is over all molecules while in $P_{w,\text{sol}}$ the largest molecule is excluded from the summation, this fact is expressed by prime at the summation sign. Before the gel point, the difference between the values of P_w and $P_{w,\text{sol}}$, decreases with an increase of the system size. In the infinite system before the gel point, P_w and $P_{w,\text{sol}}$ are identical because the contribution of the largest molecule by its weight is negligible compared to that of all other molecules. In finite systems, P_w defined above increases continuously through the gel point (in the infinite system it would diverge) and is thus of no use for detection of the gel point. On the other hand, $P_{w,\text{sol}}$, from which the contribution of the largest molecule is excluded, passes through a maximum value and decreases again. The position of maximum in the $P_{w,\text{sol}}$ (MCMS) dependence was utilized as gel point criteria;

5. Cycle rank of the network per monomer unit R . By definition R is equal to the ratio of the number of network bonds, that must be split in the gel in order to obtain a

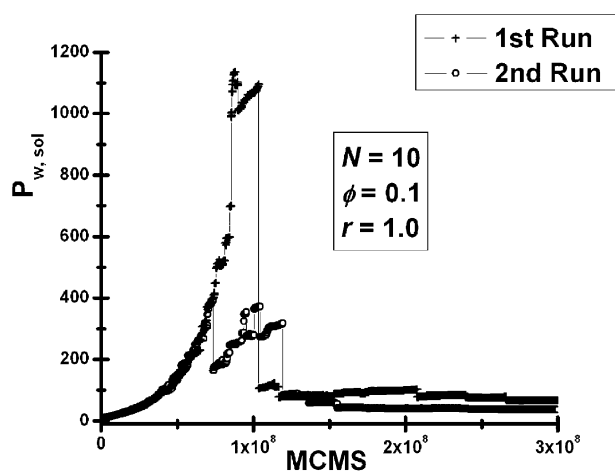


Fig. 3. Dependence of weight-average degree of polymerization excluding the largest molecule on the MCMS during two different simulation runs (initial conditions) for the system, consisting of 10-mer precursor polymer chains where $r=1.0$ and $\phi=0.1$.

spanning tree (a connected graph with a tree-like structure without cycles), to the total number of monomer units in it.

Our first goal was to find out whether the way of polymerization differs considerably as we pass from one computational run to another, i.e. from one initial configuration to the different independent one, when cross-linking parameters- N , r and ϕ are fixed. To find this out 5 independent runs (starting from different initial configuration) were carried out for several simulation systems ($N=10, 20$; $r=1.0$; $\phi=0.1, 0.4$). It turned out that at given values of ϕ , r and precursor polymer chains length N all the physical characteristics of the reacting mixture mentioned above evolve in time in the similar way for all computational runs, except for $P_{w,\text{sol}}$ (weight-average degree of polymerization excluding the largest molecule).

Fig. 3 shows two characteristic dependencies $P_{w,\text{sol}}$ (MCMS) for the system of 10-mers with $\phi=0.1$ and $r=1.0$.

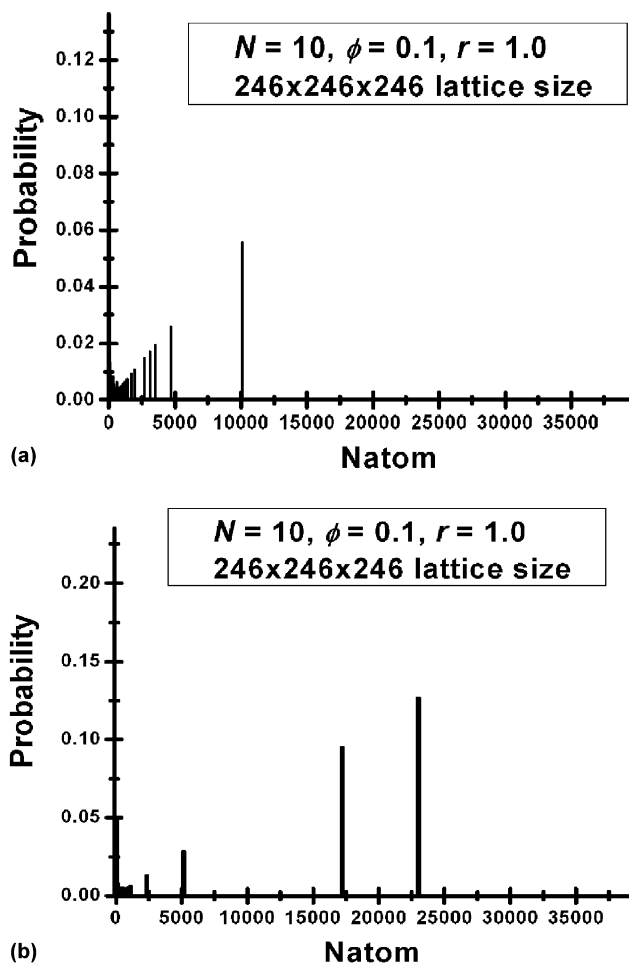


Fig. 4. Size distribution of growing molecules just before the gel point in the modeled system, consisting of 10-mer precursor polymer chains where $r=1.0$ and $\phi=0.1$ with the $246 \times 246 \times 246$ lattice size (a, for the simulation run, corresponding to the absence of sharp maximum in $P_{w,\text{sol}}$ (MCMS) dependence, b, existence of sharp maximum in $P_{w,\text{sol}}$ (MCMS) dependence).

In the first case the function $P_{w,sol}(MCMS)$ has a sharp maximum while in the second case the maximum is smoother. For all the systems studied two different scenarios of $P_{w,sol}$ time evolution (namely high and low peak in this dependence) have been observed.

To reveal the reason for this different $P_{w,sol}(MCMS)$ behaviors we have studied in detail the evolution with time of the composition of the reacting mixture. Namely, we have calculated the size distribution of growing molecules at various extents of the reaction. It appeared that there are two different ways the network formation process goes that correspond to two different $P_{w,sol}(MCMS)$ functions.

Fig. 4 shows the size distribution of growing molecules in the modeled system just before the gel point for two different scenarios of $P_{w,sol}(MCMS)$ behavior (Fig. 4a—for absence and Fig. 4b—for existence of sharp maximum in $P_{w,sol}(MCMS)$ dependence, respectively). To calculate those distributions we have chosen the configurations that were obtained, when the number of MCMS before the gel point was about the amount of monomer units and cross-linker in the modeled system. This number of MCMS is necessary for the system to reach its next configuration, since an attempt to relocate each monomer unit as well as cross-linker is made. The size distribution of growing molecules in the mixture is characterized by the probability to find a monomer in the molecule, consisting of N segments, which is equal to $P = NN_{mol}/\text{Total number of monomer units as well as a cross-linker in the modeled system}$, where N_{mol} is the number of such molecules. One should mention that Fig. 4 corresponds to the reacting mixture, consisting of 10-mer precursor polymer chains with $r=1.0$ and $\phi=0.1$ where the lattice size is $246 \times 246 \times 246$. This twice increased modeled system size was selected to avoid finite size effects.

In one case (no sharp maximum in $P_{w,sol}(MCMS)$ dependence), different molecules grow simultaneously, so that the reacting mixture remains almost homogeneous at every time step.

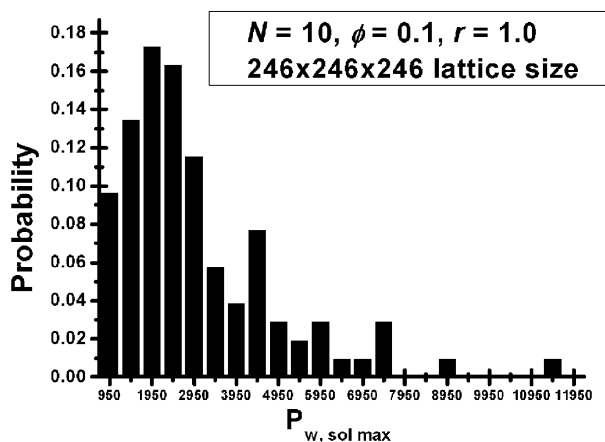


Fig. 5. The probability distribution of the value of maximum in $P_{w,sol}(MCMS)$ dependence for the simulated system, consisting of 10-mer precursor polymer chains when $r=1.0$ and $\phi=0.1$.

A considerable amount of growing molecules achieve large size before the gel point (see Fig. 4a). At the gel point they join together to form a network. One may claim that in this case polymerization resembles homogeneous gelation, during which reacting system remains almost homogeneous until the particular moment-gel point that is characterized by network formation.

In the second case (high peak in $P_{w,sol}(MCMS)$ dependence) it happens that at some point few molecules start to grow more rapidly. As a result several large colloidal particles are formed in the system before the gel point while other molecules remain relatively small (see Fig. 4b). So, one may argue that in this case network formation resembles microgel separation, when there are several large colloidal particles in reacting system, whose size and amount vary with time.

The next step was to find out whether any intermediate cases between homogeneous gelation and microgel separation could be realized in the system under consideration. That would correspond to existence of a wide range of values of the maximum in $P_{w,sol}(MCMS)$ dependence. To carry out this investigation we performed 104 independent runs for the modeled system with the size equal to $246 \times 246 \times 246$, consisting of 10-mer precursor polymer chains with $r=1.0$ and $\phi=0.1$.

Fig. 5 shows the probability distribution of the value of maximum in $P_{w,sol}(MCMS)$ dependence. One can see that indeed the value of maximum in $P_{w,sol}(MCMS)$ dependence can vary in the wide interval. However, the maximum of the distribution function is shifted towards small values of $P_{w,sol}(MCMS)$ maximum.

Further investigation showed that if $P_{w,sol \max}$ value was less than about 3000 we obtain the situation close to one when polymer network formation resembles homogeneous gelation. For $P_{w,sol \max}$ values starting from about 7000 we moved to microgel separation case. Since the most probable

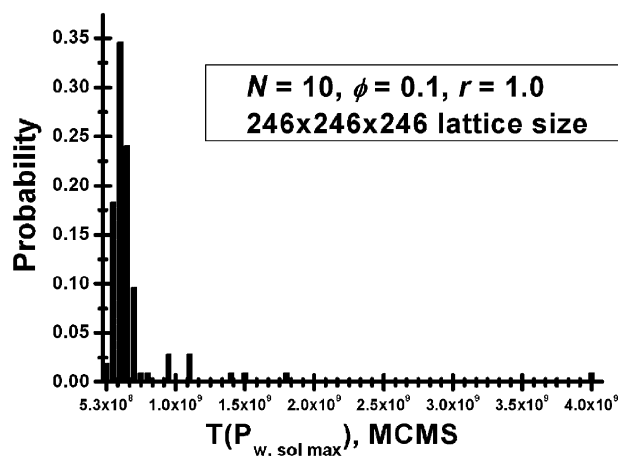


Fig. 6. The probability distribution of time when the maximum value in $P_{w,sol}(MCMS)$ dependence is achieved for the simulated system, consisting of 10-mer precursor polymer chains when $r=1.0$ and $\phi=0.1$ with the $246 \times 246 \times 246$ lattice size.

value of $P_{w, \text{sol max}}$ lies near ≈ 1950 (see Fig. 5) one may argue that network formation process goes through the homogeneous gelation more often.

Fig. 6 shows the probability distribution of time when the maximum value in $P_{w, \text{sol}}$ (MCMS) dependence is achieved. We did not find any correlations between the value of $P_{w, \text{sol max}}$ and its position. In the majority of simulations runs the maximum value in $P_{w, \text{sol}}$ (MCMS) dependence was achieved near $\text{MCMS} \approx 6.5 \times 10^8$ no matter of its magnitude.

For all the cases we have calculated final physical characteristics (fraction of unreacted chain-ends, number of segments in the largest molecule, weight-average degree of polymerization including or excluding the largest molecule and cycle rank of the network per monomer unit) of the resulting networks. It turned out that at given ϕ , r and precursor polymer chains length values all the physical characteristics of the resulting networks mentioned above differ only slightly from one simulation run to another. So, we are able to claim that gel properties are independent from initial conditions and the way the network formation goes. It means that we do not have to repeat several runs in order to measure one of the network properties.

5. Dependence of the cross-linking process on conditions of network synthesis

We have examined time evolution of the conversion of reacting solution, p , for all combinations of the studied parameters (r , ϕ , N). Fig. 7 summarizes main regularities in p (MCMS) dependences, namely, it shows the set of functions p (MCMS) for $r=0.9$ and 1.4 ; $\phi=0.1$ and 0.4 ; $N=10$ and 20 .

The first fact, which can be deduced from Fig. 7, is that in all the systems considered cross-linking process went

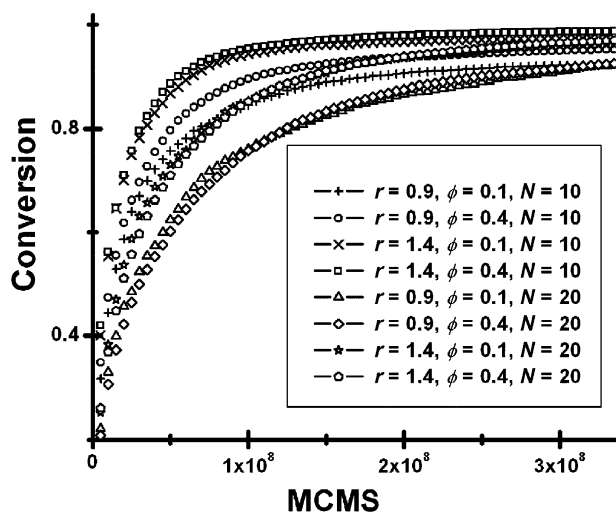


Fig. 7. Time evolution of the conversion of reacting solution at various r (0.9, 1.4), ϕ (0.1, 0.4) and N (10, 20) values.

slower as their density increased. The reason for that is a decrease of the cross-linkers and chains mobility and as a result a decrease in the effective speed of the intermolecular reactions. Moreover, one can say that the influence of ϕ on the speed of the cross-linking process is not considerable, decreasing with the length of the precursor chains growth. That is because the prevailing factor governing polymer chains mobility is not the density but the length of chains.

The main parameters that influence the speed of the molecules growth turned out to be r and N . The speed of the reaction increases monotonously with an increase of the fraction of the cross-linker (compare the curves for the lack of the cross-linkers ($r=0.9$) and for their excess ($r=1.4$)).

Considerable effect of cross-linker addition was observed for both short ($N=10$) and long ($N=20$) precursor polymer chains. It means that the effective speed of the intermolecular reactions is strongly influenced by the amount of the cross-linker.

When we used long precursor polymer chains ($N=20$) with all the other parameters (r , ϕ) fixed, the significant decrease in speed of the conversion growths was observed (see Fig. 7). For longer chains ($N=20$) it is more difficult to bend in order to form an intramolecular loop. So, one could expect an increase of the speed of the molecules growth due to the decrease of the probability of the intramolecular reactions, which do not impact into conversion. But it turned out that the decrease of the mobility of the unreacted chain ends due to the polymer chains length growth plays the major role in cross-linking process. That is why the overall speed of the network formation lowers when long precursor polymer chains ($N=20$) are used.

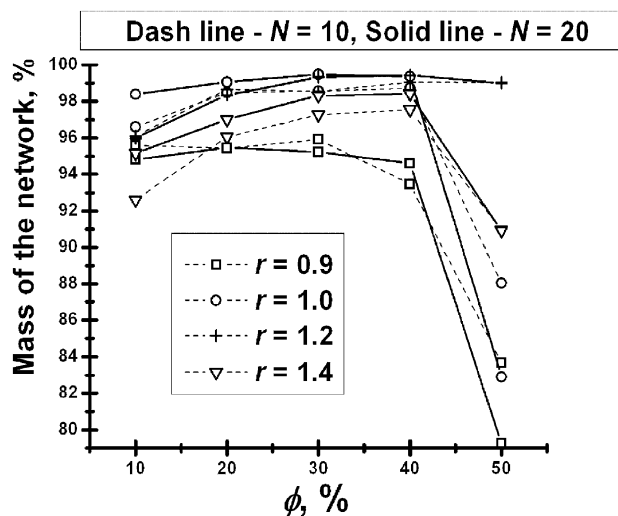


Fig. 8. The ratio between the mass of resulting network and the total mass of reacting system for different values of parameters (ϕ , r , precursor polymer chains length N) of cross-linking process.

6. Structure of the network

All the simulation runs were stopped at $\text{MCMS} = 5 \times 10^9$ (conversion ≈ 0.98) owing to the slowness of the reaction. We evaluated the structural properties of resulting networks by first determining the gel fraction. Computations that we performed for this purpose were based on the SPANFO algorithm [14]. Fig. 8 summarizes the results on the ratio between the mass of the resulting network (total number of segments in the resulting network) and the total mass of the reacting system for all considered variants of parameters of the cross-linking process.

First of all, one should stress, that the lack of cross-linker ($r=0.9$) strongly decreases the size of the resulting network no matter what ϕ and N values are. For density $\phi=0.1$ the largest gel is obtained at stoichiometric mixture composition ($r=1.0$). The use of longer chains ($N=20$) minimizes the amount of sol fraction in such systems. For density $\phi=0.2$ the largest gel molecule is also obtained at $r=1.0$ and $N=20$. If $r=1.0$ and $N=10$ or $r=1.2$ and $N=10, 20$ we obtain almost the same size of the resulting network. As the

volume fraction of monomer units of precursor chains and cross-linker molecules increases, the influence of r and N on the size of the resulting network decreases. As a result, for densities $\phi=0.3$ and $\phi=0.4$ the size of the gel is relatively the same for different r and N values with the exception of the case when we have the lack of the cross-linker ($r=0.9$).

For dense systems ($\phi=0.5$) the situation is quite different. The mass of the resulting gel changes non-monotonously with increase of the fraction of the cross-linker in the system, namely, $r=1.2$ is the optimum value to minimize the number of sol molecules after polymerization in the reacting system. The weight of soluble fraction does not depend on the precursor polymer chains length at $r=1.0$ and 1.2. As a result we obtain networks of almost the same size for $N=10$ and 20 for $\phi=0.5$ at $r=1.0$ and $r=1.2$.

Furthermore, we have developed a method to determine pendent material and amount of loops in a network. It is implemented as follows:

1. First of all a molecular graph, based on the resulting network, is constructed. Graph is a sequence of vertices,

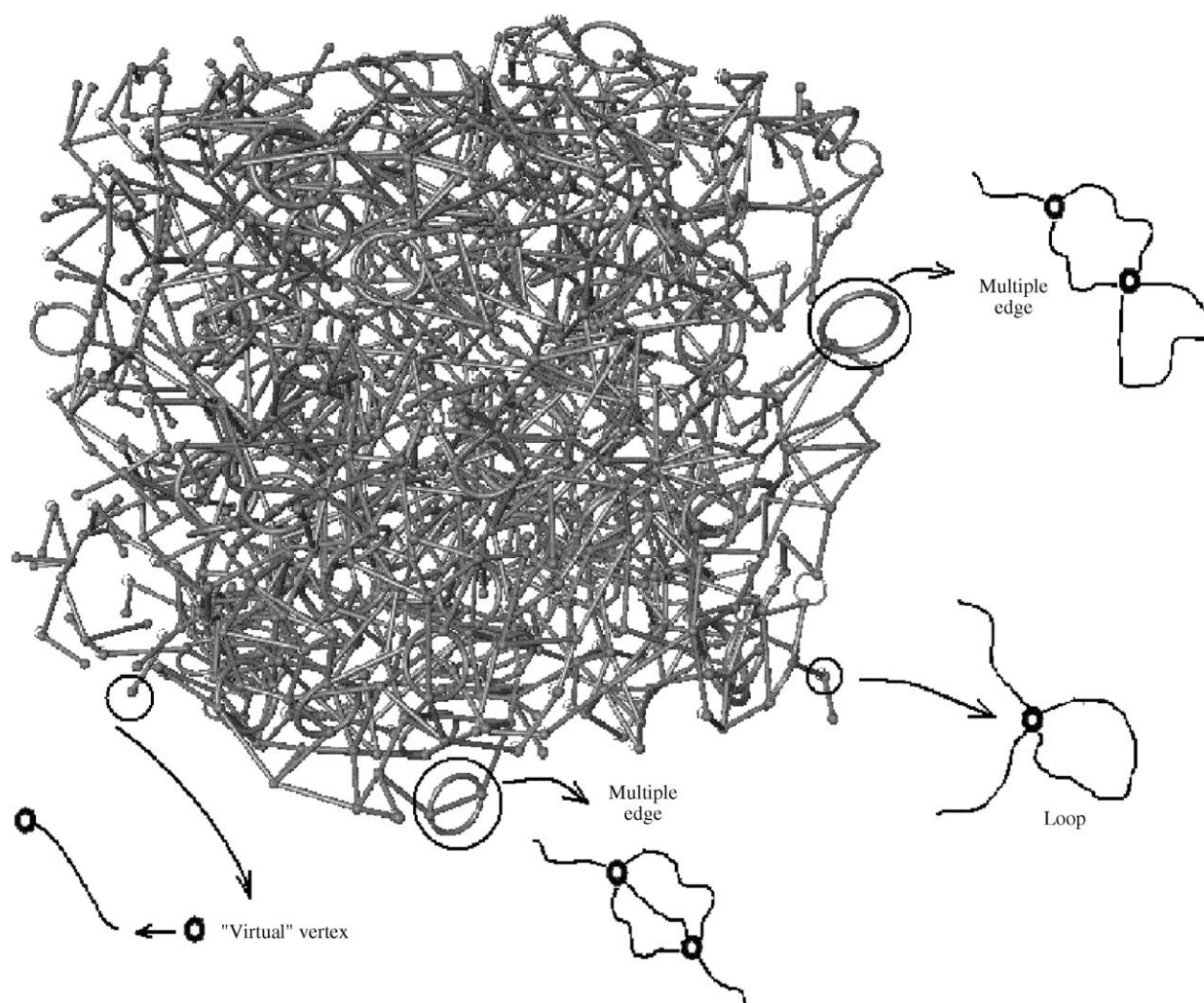


Fig. 9. Molecular graph, constructed according the network structure.

connected by a number of edges. In our case cross-links in a network are considered as vertices and polymer chains as edges. If two or three polymer chains connect the same cross-links they form single multiple edge. Those which are connected twice to the same cross-link are called loops. Besides, we had to add ‘virtual’ vertices at the end of the precursor polymer chains that are attached to the network by a cross-link at one side and do not possess it at another (the dangling terminal monomer unit of such chain is considered as vertex) in order to obtain properly constructed graph. Fig. 9 represents the resulting molecular graph, constructed for one of the obtained networks with examples for the cases that were explained above.

2. Start at each terminal point of the molecular graph—a vertex that has only one outgoing edge regardless if it is a multiple edge or a ‘virtual’ vertex. There is only one path from the terminal point to the network. All analogous vertices that have only one path to the network are considered as pendent and hence, as a part of pendent material.
3. Trace the route until a vertex is found that is not pendent. Such vertices are called elastic and are considered as the part of the elastic material. Keep track of the vertices that have been visited in order to mark them as pendent and to avoid overcounting of pendent vertices since we have to start at all terminal points.
4. At the following moment we have divided all the vertices

(cross-links in the network) into pendent and elastic ones. Now, let us turn to the edges (polymer chains in the network) that connect them.

5. All loops in the molecular graph are supposed to be a part of pendent material, no matter to which (elastic or pendent) vertex they are connected [22–24]. Edges that connect elastic vertices are considered as a part of elastic material. All the edges with at least one pendent vertex at the end are considered as a part of pendent material. The length of the precursor polymer chains is taken into consideration and the appropriate amount of monomer units (equal to the length of them) is added to the corresponding type of material. Multiple edges are added two or three times, depending on how many polymer chains they represent. One should note that the number of ‘virtual’ vertices is subtracted from the pendent material to avoid overcounting of it, since ‘virtual’ vertices are the part of polymer chains and they were counted at the step 4. Fig. 10 represents resulting division of a molecular graph into elastic and pendent parts.

Fig. 11 shows the fraction of elastic material as a function of volume fraction ϕ at different r values for two precursor polymer chain lengths N . First of all one can see that the lack of cross-linkers ($r=0.9$) strongly deteriorates elastic properties of the resulting networks. The same conclusion was made in Refs. [25,26] When there is an abundance of cross-links ($r=1.4$), the fraction of elastic

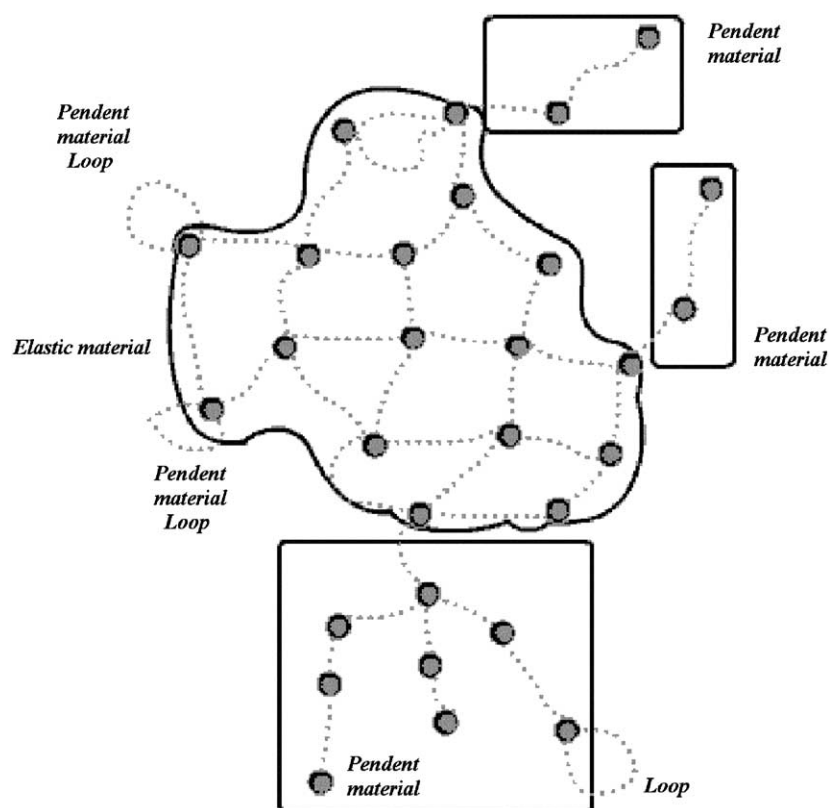


Fig. 10. The resulting division of a molecular graph into elastic and pendent parts.

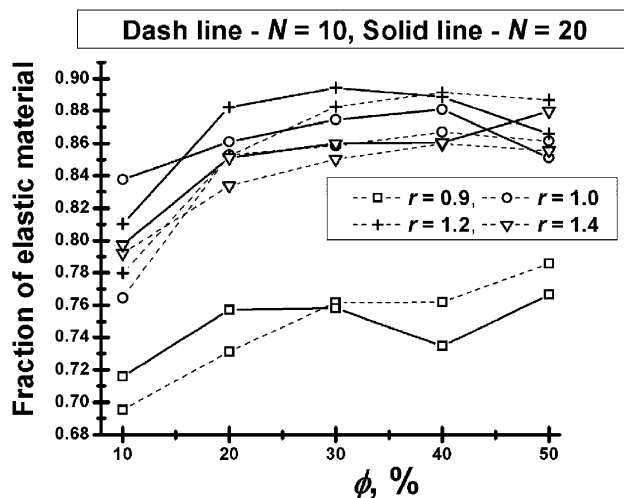


Fig. 11. The fraction of elastic material in the resulting network for different values of parameters (ϕ , r , precursor polymer chains length N) of cross-linking process.

material is much larger. The optimum network structure at which its defects are minimized is achieved at $\phi=0.3$ when $r=1.2$ and long precursor polymer chains ($N=20$) are used for cross-linking reaction. This result is in agreement with experimental observations, which show that the favorable elastic properties are achieved from long precursor polymer chains for approximately polymer melt densities at higher than stoichiometric r values [27].

As described above, pendent material of the network consists of single-chain loops and long connected pendent chains and branched pendent structures. Fig. 12 represents the dependence of the fraction of single-chain loops in the pendent material of the network on the volume fraction ϕ at different r values for both precursor polymer chains lengths N . Thus, it characterizes how the composition of the pendent material of a network depends on the parameters of cross-

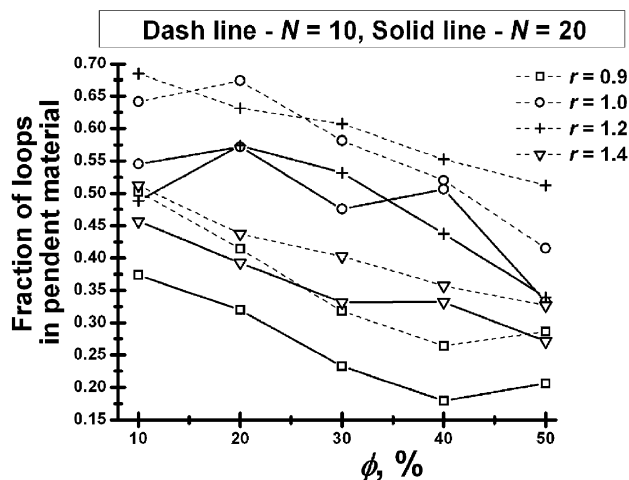


Fig. 12. The fraction of single-chain loops in pendent material of the resulting network for different values of parameters (ϕ , r , precursor polymer chains length N) of cross-linking process.

linking process. Fig. 12 shows that the lack of cross-linkers ($r=0.9$) produces dangling chains and long pendent structures, since we have a small amount of single-chain loops in the pendent material. As reacting solutions become denser, the fraction of single-chain loops decreases, and the amount of long branched pendent end-capped structures increases. Besides, for all volume fractions and r values intramolecular reactions occur more frequently with shorter chains. This results in a greater amount of single-chain loops in the pendent material for short precursor polymer chains ($N=10$) for the same other parameters of cross-linking process.

7. Conclusion

End-linked networks of 10-, 20-mer precursor polymer chains were simulated with a wide range of tetrafunctional cross-linker concentrations and polymer volume fractions using bond fluctuation model in three dimensions. It was shown that polymer network formation process can vary in the interval between homogeneous gelation and microgel separation. The amount of cross-linker and the length of precursor polymer chains are the main factors that influence the speed of cross-linking process. A method to determine soluble fraction, the amount of single-chain loops, dangling chains and branched pendent structures in polymer network was developed. For density $\phi=0.1$ the largest gel is obtained at stoichiometric ratio from long chains ($N=20$). For intermediate densities $\phi=0.2, 0.3, 0.4$ the size of resulting gel is almost the same, if we do not deal with the lack of cross-linker ($r=0.9$). For dense systems ($\phi=0.5$) $r=1.2$ is the optimum value to minimize the number of sol molecules after polymerization in reacting system. The finest elastic properties of resulting networks are achieved at $\phi=0.3$ when $r=1.2$ and long precursor polymer chains ($N=20$) are used for cross-linking reaction.

Acknowledgements

This paper is dedicated to Professor J.E. Mark on the occasion of his 70th birthday. The authors are grateful to P.G. Khalatur for helpful discussions. This work was supported by NATO 'Science for Peace' program (project SfP-977998) and Russian Foundation for Basic Research.

References

- [1] Treloar LRG. The physics of rubber elasticity. Oxford: Clarendon Press; 1975.
- [2] Erman B, Mark JE. Structures and properties of rubberlike networks. New York: Oxford University Press; 1997.
- [3] Mark JE, Erman B. Rubberlike elasticity. A molecular primer. New York: Wiley; 1988.

- [4] Mark JE. Physical properties of polymers handbook. New York: Woodbury-American Institute of Physics Press; 1996.
- [5] Mark JE, Erman B. Elastomeric polymer networks. New Jersey: Prentice Hall-Englewood Cliffs; 1991.
- [6] Mark JE, Eirich FR, Erman B. Science and technology of rubber. New York: Academic Press; 1994.
- [7] Mark JE. *Angew Makromol Chem* 1992;202(203):1.
- [8] Mark JE, Erman B. *Ann Rev Phys Chem* 1989;40:351.
- [9] Mark JE. *Macromol Symp* 2001;171:1.
- [10] Mark JE. *Macromol Chem, Phys Macromol Symp* 1996;101:423.
- [11] Mark JE. *Macromol Sci, Macromol Rep* 1995;A32:705.
- [12] Mark JE. *Comput Polym Sci* 1992;2:135.
- [13] Patel SK, Malone S, Cohen C, Gillmor JR, Colby RH. *Macromolecules* 1992;25:5241.
- [14] Nijenhuis A, Wilf HS. Combinatorial algorithms. San Diego: Academic Press; 1975.
- [15] Miller DR, Valles EM, Macosko CW. *Polym Eng Sci* 1979;19:272.
- [16] Trautenberg HL, Sommer JU, Goritz J. *Macromol Symp* 1994;81:153.
- [17] Gira N, Cohen C, Panagiotopoulos AZ. *J Chem Phys* 2000;112(15):6910.
- [18] Chen Z, Cohen C, Escobedo FA. *Macromolecules* 2002;35:3296.
- [19] Carmesin I, Kremer K. *Macromolecules* 1988;21:2819.
- [20] Deutsch HP, Binder K. *J Phys Chem* 1991;94:2294.
- [21] Trautenberg HL, Sommer JU, Goritz J. *Chem Soc Faraday Trans* 1995;91(16):2649.
- [22] Duering ER, Kremer K, Grest GS. *J Chem Phys* 1994;101:8169.
- [23] Grest GS, Kremer K. *Macromolecules* 1990;23:4994.
- [24] Grest GS, Kremer K, Duering ER. *Europhys Lett* 1992;19:195.
- [25] Leung YK, Eichenger BE. *J Chem Phys* 1984;80:3877.
- [26] Leung YK, Eichenger BE. *J Chem Phys* 1984;80:3885.
- [27] Takeuchi H, Cohen C. *Macromolecules* 1999;32:6792.